

Analyses of Fatigue Behaviour of a Low-Carbon Steel In-Air and Corrosion Medium

Aleksandar Davidkov, Donka Angelova

University of Chemical Technology and Metallurgy-Sofia, 8 Kl. Ohridski Blvd., 1756 Sofia, Bulgaria

donkaangelova@abv.bg

Key words: fatigue, corrosion, short fatigue-crack, modelling, low-carbon steel

Abstract: In-air and corrosion short fatigue crack propagation behavior of a low-carbon low-alloyed construction steel, ROLCLAS 09G2 is investigated under stress ranges $\Delta\sigma=580$ MPa and $\Delta\sigma=620$ MPa and testing frequencies $f=6,6$ Hz and $f=11$ Hz at rotating-bending, RB, conditions. The applied loading scheme is symmetric, loading ratio $R = -1$, and specimens are tested in air and in a 3,5% NaCl–water solution. The chemical composition of ROLCLAS 09G2 in wt % is as follows: C(0,09), Si(0,28), Mn(1,63), Cr(0,05), Ni(0,04), P(0,017), S(0,026), Cu(0,13), Al(0,12), As(0,014). A table model **Fatigue Rotating Bending Machine**, FATROBEM-2004 with a module for environmental assisted short fatigue crack growth investigations is designed, assembled and put in operation in the Laboratory of Plastic Deformation at UCTM-Sofia, Bulgaria. All RB fatigue tests in this study have been carried out on FATROBEM-2004.

A standard parabolic-linear model and an alternative linear model presented by a specific fatigue energy-function, both describing short fatigue crack growth behaviour of ROLCLAS 09G2 in-air and corrosion medium, have been introduced and compared. The specific band structure of ROLCLAS 09G2 makes it possible to use this steel as a modeling material in relation to composite materials.

Introduction

Generally fatigue failure occurs by propagation of subcritical cracks ranged from several microns to a few hundred microns. Those cracks are known as short cracks or small cracks which growth takes up a large percentage from the total fatigue lifetime of components and structures [1]. In this respect, the short crack effect and characterization are quite critical for accurate lifetime prediction.

In corrosion environment fatigue process depends on electrochemical, metallurgical, and mechanical factors and their interactions [2]. Thus, fatigue cracks frequently originate from pre-existing or corrosion-induced surface pits formed during exposure to service environment [3]. Such factors as frequency and fatigue waveform, strain or stress range and pit electrochemistry are also very important for crack initiation and propagation.

In the present work in-air and corrosion-assisted short fatigue crack propagation behavior in a low-carbon low-alloyed construction steel is investigated under rotating-bending symmetric loading conditions. The experimental data are described by using a unified standard parabolic-linear model and an alternative linear energy model. The results are compared for in-air and 3,5% aerated saline solution under two different frequencies and two constant-amplitude cyclic loads. A plastic replica technique is used for short fatigue crack growth monitoring.

Experimental Procedure

In-air short fatigue crack growth investigations are carried out on a table model **Fatigue Rotating Bending Machine**, FATROBEM-2004 – Fig. 1-a, [4], designed, assembled and put in operation in the Laboratory of Plastic Deformation at UCTM-Sofia. In addition a system for environmentally assisted short fatigue crack growth was fixed and corrosion fatigue tests were conducted. The main part of the fixed system is its corrosion module, shown on Fig. 2-b.

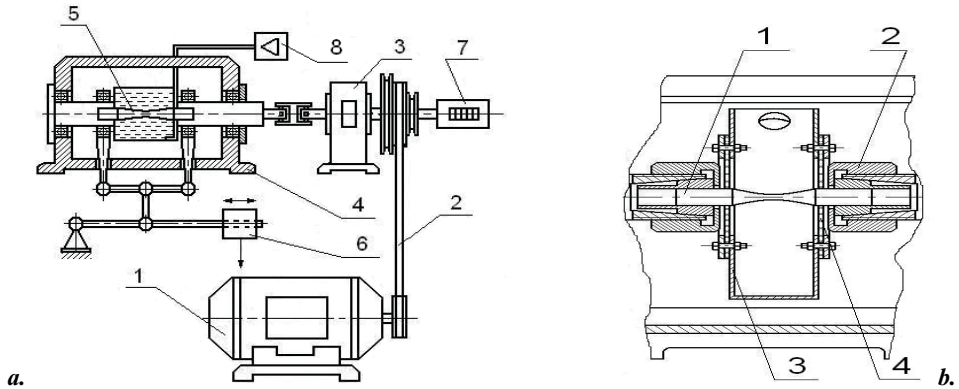


Figure 1. Table model of fatigue machine FATROBEM-2004:

- a.** Whole machine – electric engine 1, driving belt 2, ball-bearing unit 3, testing box 4, specimen 5, device for loading 6, counter 7, device for circulation and aeration of corrosion agent 8;
- b.** Corrosion module of fatigue machine – specimen 1, clutch joint 2, corrosion cell 3, rubber gasket 4

The steel under investigation is a rolled low-carbon, low alloyed steel, ROLCLAS, marked as 09G2 according to the Bulgarian Construction Steel Standard, mostly used for off-shore applications and in shipbuilding. The chemical composition and the mechanical properties of ROLCLAS 09G2 steel are shown in Table 1. The average ferrite grain size is $d = 25.6 \mu\text{m}$.

Chemical Composition, wt %												
Steels	C	Si	Mn	Cr	Ni	P	S	Cu	Al	As	Mo	V
ROLCLAS-09G2	0.09	0.28	1.63	0.05	0.04	0.017	0.026	0.13	0.12	0.014	–	–
Mechanical Properties												
Steels	Tensile Strength σ_B [MPa]		Proof strength $\sigma_{0.2}$ [MPa]			Cross section contraction ψ , [%]		Hardness HB [MPa]	Average grain size [μm]			
ROLCLAS-09G2	475.3		382			62.3		148	25			

Table 1. Characteristics of ROLCLAS 09G2 steel

Steel ROLCLAS 09G2 is available as rolled sheets of 8 mm thickness. Its microstructure reveals a sequence of long and uniform pearlite and ferrite bands, as shown in Fig. 2, [5].

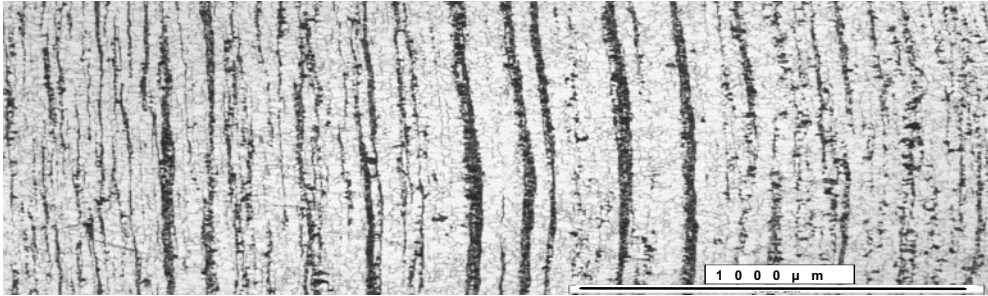


Figure 2. Microstructure of ROLCLAS 09G2 steel – cross section view

In-air and corrosion fatigue tests used the same specimens of smooth hour-glass type. The specimen surface was properly polished according to the corresponding technical standards. All experiments employed the Method of Short Fatigue Crack Growth and crack propagation was monitored by surface replicas. The replicas were taken during fixed intervals of the cyclic loading and recorded the surface specimen's state and fatigue crack length. The replicas were examined later by light microscope in order to find crack initiation and propagation and to measure cracks' sizes.

The first set of experiments are carried out on FATROBEM–2004 in air and in aerated saline solution under symmetric rotating-bending, RB, $R = -1$ at different cyclic frequency and loading conditions presented in Table 2.

ROLCLAS 09G2				
Rotating-bending at $R = -1$ in air and in aggressive environment of NaCl solution				
No	Stress range MPa	Frequency Hz	Environment	Lifetime cycles
1	620	11	air	106700
2	580	11	air	132990
3	580	11	air	310420
4	620	6,6	air	86570
5	580	6,6	3,5% NaCl	80740
6	580	11	3,5% NaCl	30360
7	620	6,6	3,5% NaCl	41800
8	620	11	3,5% NaCl	16600

Table 2. Experimental conditions and fatigue lifetimes

Results, analyses and discussion

Data obtained from fatigue in air and aggressive environment – crack lengths a , μm and the corresponding numbers of cycles N , cycles – are plotted as “Crack length, a –number of cycles, N ” and shown in Fig. 3 and Fig. 4.

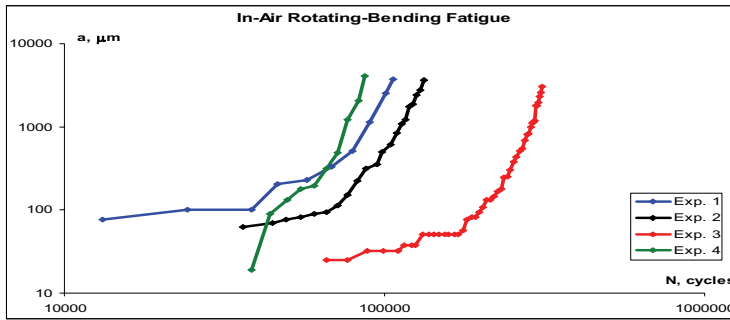


Figure 3. Dependence “Crack length, a - number of cycles, N ”

In Fig. 4, it can be seen all main cracks propagating on the specimen surfaces. The specimen from experiment 3, subjected to the lowest stress level $\Delta\sigma=580\text{MPa}$ shows the longest lifetime, $N=310420$ cycles. The main crack starts propagating much later in comparison to the main cracks of the other specimens. Its initial length is found to be $25\mu\text{m}$ at 66 000 cycles (comparatively late) and its growth as a short crack takes 78,73 % of the whole fatigue lifetime. The corresponding crack parameters of the other specimens tested at the highest stress level of 620MPa are respectively: for experiment 1 – $76\mu\text{m}$ at 13 200 cycles, when it takes 87,62 % of the whole lifetime; and for experiment 2 – $63\mu\text{m}$ at 30470 cycles and 77,61% of the whole lifetime. After the transition “short-long crack” all cracks show similar behaviour as their curves develop almost in parallel up to failure. However, the specimen 4 shows an exception concerning the already involved crack parameters – $19\mu\text{m}$ at 38 500 cycles and 55,5 % of the whole lifetime at almost vertical development of its crack curve. This particular specimen was tested at a frequency of 6,6Hz, while all the others had experienced a frequency of 11Hz. No specific difference had been found between the surface of specimen 4 and that of the remaining specimens.

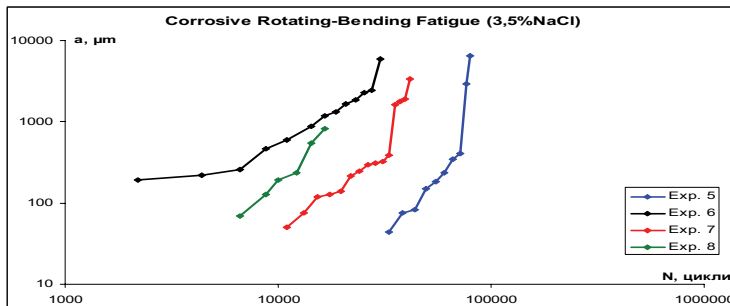


Figure 4. Dependence “Crack length, a - number of cycles, N ”

In Fig. 5, also is shown the main cracks behaviour, but for all experiments carried out in air and in a 3,5% aerated saline solution. The longest lifetime belongs to the specimen 5, subjected to stress level $\Delta\sigma=580\text{MPa}$ and frequency of 6,6Hz. The main crack here starts propagating at 33000 cycles and its initial length is found to be $44\mu\text{m}$. The specimen failed at 80740 cycles and the growth of the main crack as a short one takes 58,6% of the whole fatigue lifetime. As it was already mentioned, the longest fatigue lifetime belongs to the specimen from experiment 5, carried out at the lower loading frequency. It is in contradiction with an expected behaviour at which a lower frequency causes an earlier failure in aggressive environment. However, the number of performed experiments is not enough, the difference between the applied frequencies is not large and the stress

levels in use are comparatively high in order to make some general conclusions about duration of fatigue lifetime. The specimen from experiment 6 ($\Delta\sigma=580\text{MPa}$) has long scratch on its surface ($244\mu\text{m}$) obviously not removed during the polishing process. That scratch had become a starting point for a fast growing main crack initiated at 2200 cycles and caused specimen failure at 30360 cycles. But the lifetime of specimen 6 is still longer than that of specimen 8 which failed at 18700 cycles, possibly because of the higher stress level $\Delta\sigma=620\text{MPa}$.

A comparison of the main cracks' behaviour for in-air and corrosion assisted fatigue presented in Fig. 5 shows earlier formation of cracks and earlier failure of specimens subjected to fatigue loading in aggressive environment.

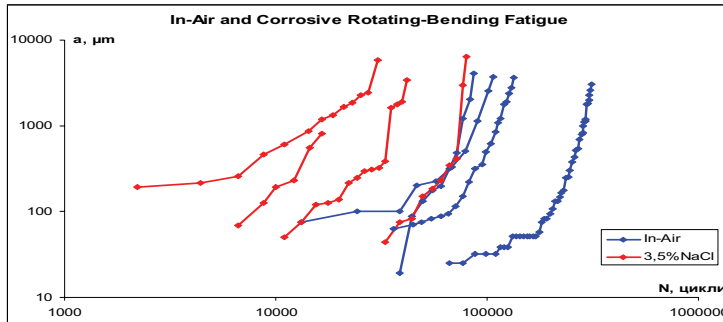


Figure 5. Dependence “Crack length, a - number of cycles, N ” in different environments

For all data presentations we use parabolic-linear mathematical model “Crack growth rate, da/dN – crack length a ” at cyclic RB loading – Eq. (1) – based on some investigations made in [6, 7]. The model comprises description of fatigue crack growth behaviour in its three different stages (I. Stage of short fatigue crack growth (SFC), II. Stage of physically small fatigue crack growth (PhSFC), III. Stage of long fatigue crack growth (LFC)) and analytical determination of the characteristics dividing those three stages and known as microstructural barriers d_1 and d_2 , at which cracks are slowing down and stop; the other model parameters include a_0 and a_f – the initial and final crack sizes, and A, B, C – material constants.

$$\text{M: } \begin{cases} \text{I(SFC): } \left(\frac{da}{dN}\right)_{sh} = A_1 a^2 + A_2 a + A_3, a \in [a_0, d_1] \\ \text{II(PhSFC): } \left(\frac{da}{dN}\right)_{phs} = B_1 a^2 + B_2 a + B_3, a \in [d_1, d_2] \\ \text{III(LFC): } \left(\frac{da}{dN}\right)_l = C_1 a^{C_2}, a \geq d_2 \end{cases} \quad (1)$$

The mathematical model is applied only to the main cracks observed on the specimens although usually most of those specimens have more than one crack. The values of the essential microstructural barriers d are determined by an algorithm proposed in [8]. For in-air crack propagation those barriers are calculated as $d_1=230\mu\text{m}$, $d_2=565\mu\text{m}$ and for corrosion assisted crack propagation – as $d_1=175\mu\text{m}$, $d_2=332\mu\text{m}$.

The graphical presentation of the mathematical model can be seen in Fig. 6: in Fig. 6–*a* for in-air RB fatigue; and in Fig. 6–*b* for corrosion assisted RB fatigue.

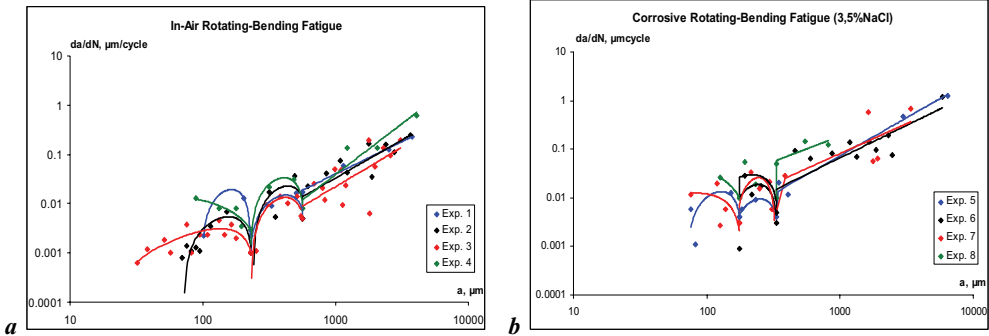


Figure 6. Presentation “Crack length, a - number of cycles, N ” at RB fatigue in different environments:
a. in-air fatigue; **b.** in corrosion fatigue

From Fig. 6–*a* is clear that during the first stage of crack propagation, *SFC*, the highest growth rate belongs to the specimen from experiment 1, while during the stages of physically small, *PhSFC*, and long, *LFC*, fatigue crack development, the highest growth rate belongs to the specimen of experiment 4. At the same time the lowest growth rate for all stages and all specimens belongs to the main crack from experiment 3. In Fig. 6–*b* the maximum crack growth rate during all the three stages belongs to the main crack from experiment 8, while the lowest crack growth rate during *SFC* stage belongs to the main crack from experiment 7 and during the *PhSFC* stage – to that from experiment 5. The main crack from experiment 6 starts from a scratch longer than d_i and that is why we do not have any data for *SFC* growth of that crack.

Figure 7 presents both *Families of parabolic-linear curves*, respectively **blue** for in-air fatigue and **red** for fatigue in aggressive environment. An analysis of Fig. 7 shows higher growth rate in the case of corrosion assisted crack development in comparison with in-air crack propagation. Also we can see some narrowing of *PhSC* stage and a shifted beginning of *LFC* stage to a lower number of fatigue cycles. All that confirms the fact that the aggressive medium accelerates fatigue crack growth sufficiently. However, such a medium mainly helps cracks to grow easier in depth and leads to location of their surface growth data relatively closer to in-air fatigue crack growth data.

An alternative approach to already described classical way of treating fatigue comprises a new specific fatigue energy-function W , and a new presentation of experimental data in parameters dN/da , ΔW . The function ΔW discussed for the first time in Angelova [9, 10] has a dimension of surface energy per second and unity of crack size, and leads to a *Linear presentation of fatigue data* that is $da/dN - \Delta W \rightarrow$ Lines ΔW_a and ΔW_c shown as thick lines in Fig. 8, which correspond respectively to in-air fatigue and fatigue in corrosive environment. The scatter band is indicated by two thin lines at a condition of excluding two distant points from the Line ΔW_a ; the thin lines correspond to $1/2$ and 2 folds of da/dN .

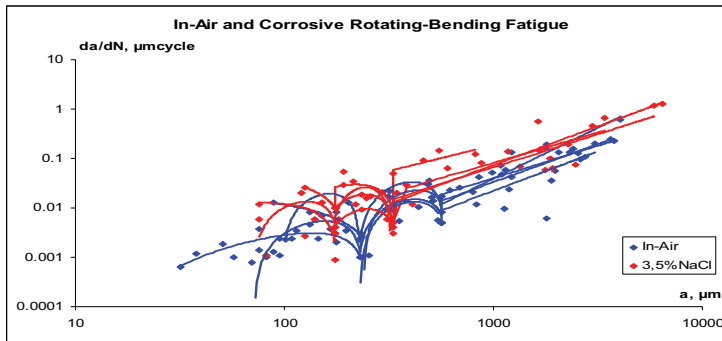


Figure 7. Comparison between presentations “Crack length, a - number of cycles, N ” at RB fatigue in different environments

Such a precision gives us possibilities to use the presentation $da/dN-\Delta W$ at lesser number of measurements-recordings under every fatigue test, especially at such a higher correlation coefficient $f_{cor}>0.8$. Afterwards a transition to the presentation “ $da/dN - a$ ” showing much larger scatter would not be difficult.

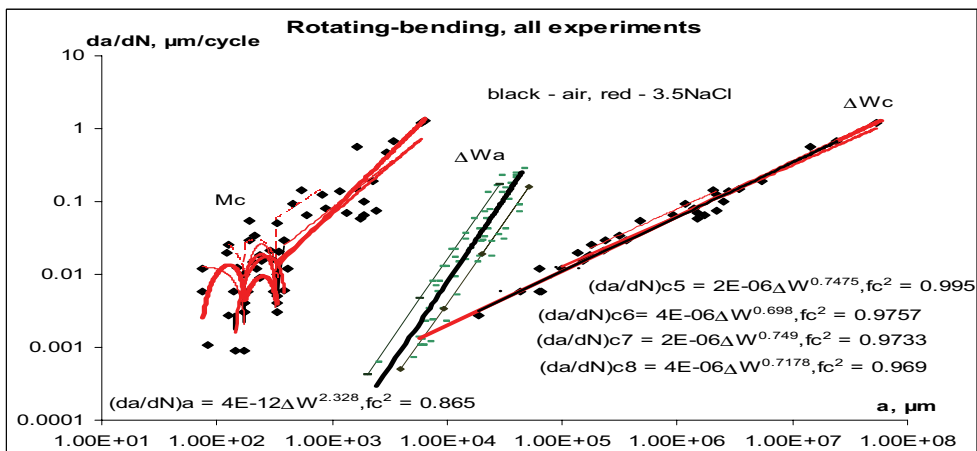


Figure 8. Different presentation of fatigue data:

a. Parabolic-linear family “Crack growth rate, da/dN – crack length, a ”, respectively M_c for corrosion fatigue;

b. Linear families “Crack growth rate, da/dN – Surface energy ΔW ”, respectively the Line ΔW_a for in-air fatigue and the Linear family ΔW_c for corrosion fatigue

The alternative linear presentation of in-air and corrosion fatigue data, $da/dN-\Delta W$ may be treated as *natural fatigue tendency* of material at a given stress range and environment.

Summary

The proposed Parabolic-linear mathematical model can describe and predict adequately short crack behaviour under rotation-bending fatigue in air and in aggressive environment. This is additionally

supported by the comparison of predicted and actual fatigue lifetimes. An attempt is made to fit rotation-bending fatigue data obtained in air and in corrosion medium into a Linear presentation based on a specific fatigue energy-function, which after some more data and proves can be found useful for fatigue testing practice. The line obtained by the Linear presentation may be called *natural fatigue tendency* of a given material in a given environment.

Acknowledgements. The authors thank the Ministry of Education and Science and the University UCTM in Bulgaria for their valuable support on Contracts: TH-102; 10499,10500.

References:

- [1] S. Suresh, *Fatigue of Materials*, Cambridge University Press-UK, Cambridge, (1998).
- [2] D.V. Ramsamoj, T.A. Shugar, Modeling of corrosion fatigue in metals in an aggressive environment. *International Journal of Fatigue* 23 (2001) S301–S309
- [3] F. Plessier, N. Saintier, I. Aubert, J.M. Olive, J.P. Frayret, Experimental and Numerical Investigation of the Effect of Pitting on Microplasticity Development Under Fatigue Loading in a 316L Austenitic Stainless Steel., In *Proceedings of 9-th international fatigue congress*, CD-ROM, Atlanta, USA (2006)
- [4] D. Angelova, A. Davidkov, Modelling of short crack growth in a low carbon steel, subjected to rotation-bending fatigue. In *Proceedings of the 16th European Conference of Fracture, Failure Analysis of Nano and Engineering Materials and Structures*, Alexandroupolis, Greece (2006)
- [5] A. Davidkov, R. Pippa, Studies on short fatigue crack propagation through a ferrite-pearlite microstructure., In *Proceedings of the 9-th International Fatigue Congress*, CD ROM, Atlanta, Georgia, USA (2006)
- [6] R. Yordanova, Modeling of fracture process in a low-carbon 09Mn2 steel on the bases of short fatigue crack growth experiments. Comparative analyses on the fatigue behaviour of other steels. PhD Thesis, University of Chemical Technology and Metallurgy – Sofia (in Bulgarian) (2003)
- [7] D. Angelova, A. Davidkov, Different analytical presentations of short crack growth under rotation-bending fatigue., In *Proceedings of the 16-th European Conference of Fracture, Failure Analysis of Nano and Engineering Materials and Structures*, CD ROM, Alexandroupolis, Greece (2006), pp 175-176
- [8] A. Davidkov, *On factors influencing fatigue in 09Mn2 steel*. PhD Thesis, University of Chemical Technology and Metallurgy – Sofia (in Bulgarian), (2006)
- [9] D. Angelova, , In *CD Proceedings of ECF13, Abstracts*, San Sebastian, Spain, September (2000), p.128.
- [10] D. Angelova, In *Proceedings of the ECF14*, Vol. 1, Cracow, Poland, September (2002), pp.89-97.